

Effect of the Carboxylate Shift on the Reactivity of Zinc Complexes in the Gas Phase

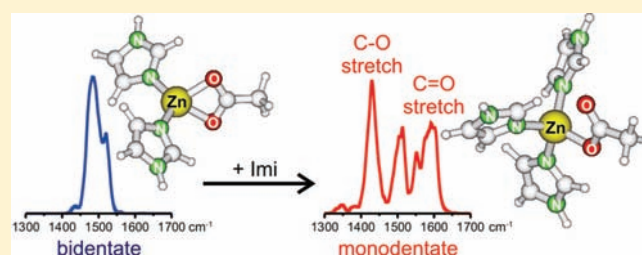
Lucie Ducháčková,[†] Detlef Schröder,[‡] and Jana Roithová^{*,†}

[†]Department of Organic Chemistry, Charles University in Prague, Hlavova 8, 12843 Prague 2, Czech Republic

[‡]Institute of Organic Chemistry and Biochemistry, Academy of Sciences of the Czech Republic, Flemingovo náměstí 2, 16610 Prague 6, Czech Republic

S Supporting Information

ABSTRACT: The effect of different modes of the carboxylate ligands on the reactivity of gaseous zinc–acetate complexes is reported. Using infrared multiphoton dissociation spectroscopy, it is demonstrated that the coordination of acetate in $[(\text{Imi})_n\text{Zn}(\text{CH}_3\text{COO})]^+$ complexes (Imi = imidazole, $n = 1-3$) changes from bi- to monodentate upon coordination of the third imidazole ligand. This so-called carboxylate shift substantially influences the reactivity of the zinc–acetate complexes in comparison to complexes with monodentate counterions. The differences in reactivities are demonstrated on the ligand exchange reactions of $[\text{L}_n\text{ZnX}]^+$ ($n = 2$ or 3 ; $\text{L} =$ imidazole or pyridine; $\text{X} = \text{OH}, \text{Cl}, \text{CH}_3\text{COO},$ and CH_3CONHO).



INTRODUCTION

The zinc cation is one of the most common metals in the active centers of metalloenzymes. In contrast to most other transition metals in metalloenzymes, zinc usually does not undergo redox reactions but instead serves as a binding site for the appropriate activation and geometrical arrangement of the reactants. The possible number of ligands around the zinc ion in a constrained environment of an enzyme molecule ranges from three to six.^{1–3} The most often involved reactant in the reactions catalyzed by zinc-containing enzymes (catalytic sites) is the water molecule. Scheme 1 shows a carboxypeptidase as an example, in which the water ligand serves in the hydrolysis of a peptide bond.^{1,4} Zinc is surrounded by water, two histidine residues, and a carboxylate function of glutamate, which is coordinated as a monodentate ligand. The release of the water molecule is assisted by a change of the coordination of the carboxylate toward the bidentate mode. This flexibility of the carboxylate coordination, which assists the reactivity at the catalytic centers in zinc enzymes, is referred to as a carboxylate shift.^{5–7}

Outside the restricted enzyme environment, zinc cations are usually tetraordinated, but also higher coordination numbers are possible. For example, using quantum-chemical methods and their combinations with molecular modeling, it has been concluded that Zn^{2+} ions are, in water solutions, mostly hexacoordinated.⁸ However, with stronger bound ligands, for example ammonia, or when one of the ligands is an anion, the coordination number changes to four.⁹ Thus, the first solvation shell of $\text{Zn}(\text{OH})^+$ contains three molecules of water, and additional water molecules bind already to a second solvation shell.^{10,11} The situation is thus analogous to the biological systems, in which the

zinc ion is bound to glutamate or aspartate and three additional ligands.¹²

The aim of this paper is to investigate the effect of counterions in zinc complexes on the association and dissociation of ligands, with a particular focus on the role of the carboxylate shift. Complexes of zinc acetate, zinc chloride, zinc hydroxide, and zinc acetohydroxamate with two or three imidazole or pyridine ligands are taken as models for spectroscopic investigations and reactivity studies in the gas phase.

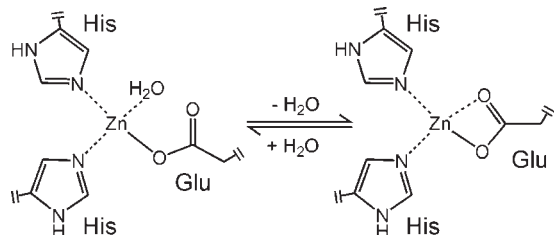
EXPERIMENTAL AND COMPUTATIONAL DETAILS

The collision-induced dissociation (CID) experiments were performed with a TSQ 7000 mass spectrometer with a QOQ configuration (Q stands for quadrupole and O stands for octopole) described in detail elsewhere.¹³ The ions of interest were generated by electrospray ionization (ESI) from either an aqueous solution of ZnCl_2 or $\text{Zn}(\text{CH}_3\text{COO})_2$ and imidazole or D_5 -pyridine (perdeuterated pyridine). The first quadrupole was used to record source spectra or to mass-select the desired ions. The mass-selected ions were reacted with pyridine at variable pressures in the octopole collision cell, and the ionic products were analyzed by Q2. The collision energy was varied by changing the potential offset between Q1 and O. The nominal zero collision energy was determined using a retarding potential analysis¹⁴ (see Figure S1 in the Supporting Information), and the energy resolution was 1.2 ± 0.1 eV in the laboratory frame (full width at half-maximum). All results are averages of at least two independent measurements. It is to be noted that the reactant ions emerging from the ESI source were not thermalized,¹⁵

Received: February 9, 2011

Published: March 07, 2011

Scheme 1. Illustration of the Carboxylate Shift Assisting Dissociation/Association of a Water Ligand to Zinc in the Active Center of an Enzyme



but as identical experimental settings were used for all ions, we assume that the reactivities are comparable.

The gas-phase infrared (IR) spectra of mass-selected ions were recorded using a Bruker Esquire 3000 ion trap mounted to a free electron laser at CLIO (Centre Laser Infrarouge Orsay, France).¹⁶ The free electron laser (FEL) was operated in the 40–45 MeV electron-energy range, and it provided light in the 1000–1800 cm^{-1} range. The relative spectral line width of the FEL is about 1%, and the precision of the measurement of the wavenumbers with a monochromator is about 1 cm^{-1} . Each point in a raw spectrum is an average of 32 measurements. The ions were generated by electrospray ionization as described above. The ions were mass-selected and stored in an ion trap. The fragmentation was induced by four laser macropulses of 8 μs admitted to the ion trap, and the dependence of the fragmentation intensities on the wavelength of the IR light gives the infrared multiphoton dissociation (IRMPD) spectra. The reported IRMPD spectra are averages of two raw spectra and are not corrected for the power of the free-electron laser, which slightly changes dependent on the wavenumbers (see the Supporting Information). The spectrum of $[(\text{Imi})\text{Zn}(\text{CH}_3\text{COO})]^+$ was measured with the full power of the FEL, whereas one attenuator was used for the spectrum of $[(\text{Imi})_2\text{Zn}(\text{CH}_3\text{COO})]^+$ and two attenuators of the laser power were used for the spectrum of $[(\text{Imi})_3\text{Zn}(\text{CH}_3\text{COO})]^+$.

The computational density functional theory (DFT) study¹⁷ was performed using the B3LYP^{18–21} together with the TZVP basis set as implemented in the Gaussian 03 package.²² All minima were identified by the analysis of the Hessian matrix. Several possible geometries for each complex were optimized, and the results refer to the most stable isomers/conformers that were identified. All energies given below refer to 0 K (energies are sums of total energies and zero-point vibrational energies). The calculated frequencies were scaled by a factor of 0.986, which leads to the overall best agreement between theory and experiment using a single scaling factor for all spectra studied here (cf. below).²³ All optimized structures and their energies are given in the Supporting Information.

RESULTS AND DISCUSSION

A prerequisite of our study is the determination of the binding modes of acetate in the zinc complexes with two and three additional ligands. While generally the conservation of a 4-fold zinc coordination and thus a change of bidentate coordination of acetate in $[\text{L}_2\text{Zn}(\text{CH}_3\text{COO})]^+$ to monodentate in $[\text{L}_3\text{Zn}(\text{CH}_3\text{COO})]^+$ might be expected, there are reports showing also higher coordination numbers of zinc.^{24–27} We have therefore investigated the ion structures of zinc–acetate cations with different numbers of ligands by means of infrared multiphoton dissociation spectroscopy (IRMPD). As a model system, we have chosen $[(\text{Imi})_n\text{Zn}(\text{CH}_3\text{COO})]^+$ with $n = 1–3$.

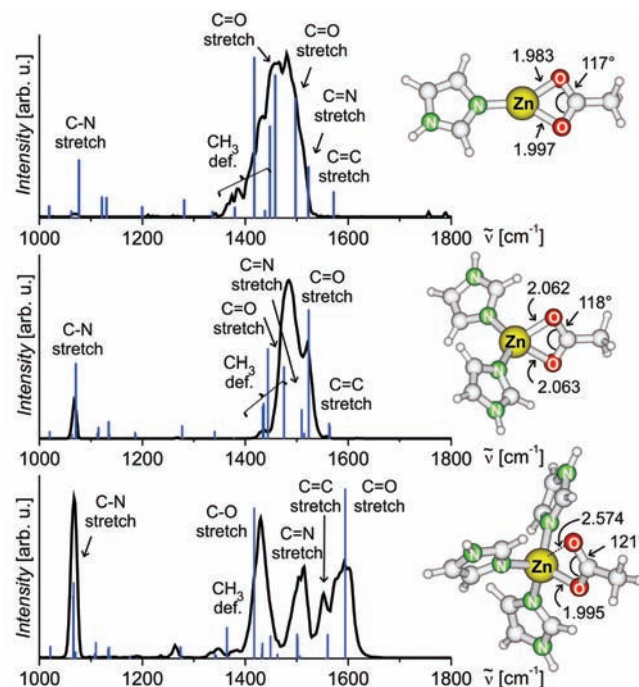


Figure 1. Experimental IRMPD spectra and theoretical IR spectra of (a) $[(\text{Imi})\text{Zn}(\text{CH}_3\text{COO})]^+$, (b) $[(\text{Imi})_2\text{Zn}(\text{CH}_3\text{COO})]^+$, and (c) $[(\text{Imi})_3\text{Zn}(\text{CH}_3\text{COO})]^+$. The structures show the computed minima for the corresponding ions with selected bond lengths given in Ångströms.

The IRMPD spectra of the $[(\text{Imi})_n\text{Zn}(\text{CH}_3\text{COO})]^+$ complexes show a striking difference between $n = 1$ and 2 on one hand and $n = 3$ on the other (Figure 1). The spectra of the former ions are dominated by a composite band centered slightly below 1500 cm^{-1} . On the contrary, the spectrum of $[(\text{Imi})_3\text{Zn}(\text{CH}_3\text{COO})]^+$ is much more structured in this particular spectral region. Specifically, two new bands appear at roughly 1400 cm^{-1} and 1600 cm^{-1} . This finding demonstrates that the coordination of a third imidazole molecule to the zinc–acetate ion has a substantial effect on the coordination of the acetate anion.²⁸

We have performed complementary density functional theory calculations in order to explain the ligand effect and also unravel the identity of the individual bands in the IRMPD spectra. The theoretical infrared spectra for the most stable isomers of the investigated ions agree very well with the experimental IRMPD patterns. The wide bands at roughly 1500 cm^{-1} in the spectra of $[(\text{Imi})\text{Zn}(\text{CH}_3\text{COO})]^+$ and $[(\text{Imi})_2\text{Zn}(\text{CH}_3\text{COO})]^+$ correspond to the CO and CN stretching modes with a possible contribution of C–H deformation vibrations at lower wavenumbers. The splitting between the symmetric and the antisymmetric C=O stretching modes of carboxylate amounts to about 40 cm^{-1} .

The most stable arrangement of $[(\text{Imi})_3\text{Zn}(\text{CH}_3\text{COO})]^+$ contains a monodentate coordination of the acetate ligand, which results in the appearance of two new bands at roughly 1417 cm^{-1} and 1595 cm^{-1} . The band at the lower wavenumbers corresponds to the vibration of the C–O single bond coordinated to zinc, whereas the band at 1595 cm^{-1} represents the vibration of the carbonyl group. The carbonyl band is red-shifted with respect to typical carbonyl bands in carboxylic acids ($\sim 1700 \text{ cm}^{-1}$), which is the result of a weak interaction with zinc (the distance between carbonyl oxygen and zinc amounts to

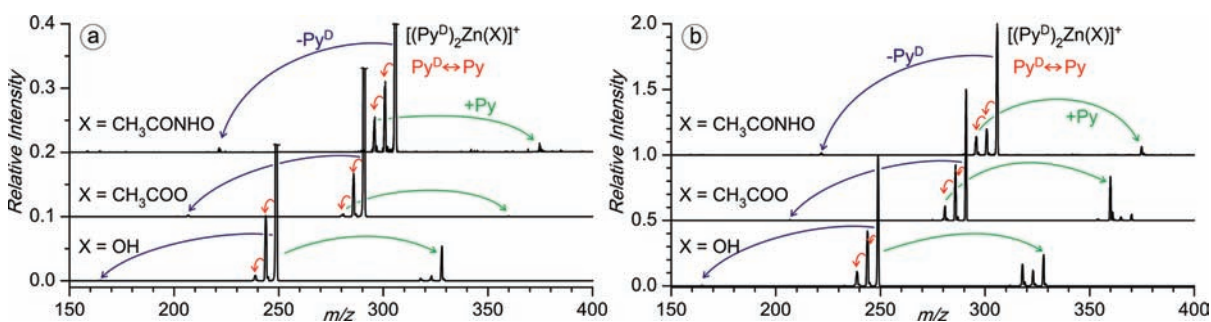


Figure 2. Reaction between $[(\text{Py}^{\text{D}})_2\text{ZnX}]^+$ ($\text{X} = \text{OH}$, CH_3COO , and CH_3CONHO) and unlabeled pyridine at (a) a lower pressure ($p_{\text{Py}} \sim 0.01$ mtorr) and (b) a higher pressure ($p_{\text{Py}} \sim 0.1$ mtorr). The spectra are normalized by setting the parent-ion intensity to 1.0 (note that the parent peaks in part a are off scale).

2.574 Å). The C=N stretching mode stays at $\sim 1500\text{ cm}^{-1}$, and a band at 1550 cm^{-1} we assign to the C=C stretching. In addition, the spectra contain a sharp band at $\sim 1070\text{ cm}^{-1}$, which represents a stretching mode of a single C–N bond.

Notably, the IRMPD spectrum of $[(\text{Imi})_3\text{Zn}(\text{CH}_3\text{COO})]^+$ agrees best with the theoretical IR spectrum, in that we can see also the C=C stretching band, which is completely missing in the spectra of $[(\text{Imi})\text{Zn}(\text{CH}_3\text{COO})]^+$ and $[(\text{Imi})_2\text{Zn}(\text{CH}_3\text{COO})]^+$ (see Figure 1). The reason can stem from a larger energy required for the fragmentation of the latter complexes, which means that more IR photons have to be absorbed in order to induce the fragmentation. The best agreement between an IRMPD spectrum and an IR spectrum would be expected, if absorption of only one IR photon would be sufficient for inducing the fragmentation. The increased amount of necessary photons can be reflected in a nonlinear response of individual absorption bands in the resulting IRMPD spectrum. The same reasoning can be offered for the different sensitivity of the C–N stretching mode (see Figure 1).

In summary, the IRMPD study provides clear evidence that the coordination of acetate in $[(\text{Imi})_n\text{Zn}(\text{CH}_3\text{COO})]^+$ experiences a substantial change upon coordination of a third ligand to the zinc ion, which can be viewed as a gas-phase mimic²⁹ of the carboxylate shift in biochemistry.

In the following, we address the question of whether the flexibility in coordination of acetate brings an advantage for the reactivity of zinc complexes or whether the reactivity of analogous complexes with different counterions is analogous. Possible effects of the counterions are first investigated in a thermoneutral reaction of $[(\text{Py}^{\text{D}})_n\text{ZnX}]^+$ with pyridine (Py), where Py^{D} is D_5 -pyridine; n is 2 or 3; and X is OH, Cl, CH_3COO , or CH_3CONHO . Hydroxide and chloride are taken as representatives of monodentate counterions, whereas the acetohydroxamate stands for a typical bidentate counterion.^{13,30} The reactions were performed at nominally zero collision energy and at two different pressures (even only traces of pyridine at the background pressure lead already to multiple reactions; cf. Figure S2 in the Supporting Information). Figure 2 illustrates the reactions of $[(\text{Py}^{\text{D}})_2\text{ZnX}]^+$ ($\text{X} = \text{OH}$, CH_3COO , CH_3CONHO) at two different pressures of pyridine. The results at the lower pressure (Figure 2a) show a distinct difference between $[(\text{Py}^{\text{D}})_2\text{ZnOH}]^+$ on one hand and $[(\text{Py}^{\text{D}})_2\text{Zn}(\text{CH}_3\text{COO})]^+$ and $[(\text{Py}^{\text{D}})_2\text{Zn}(\text{CH}_3\text{CONHO})]^+$ on the other. For the $[(\text{Py}^{\text{D}})_2\text{ZnOH}]^+$ ion, the rates of the exchange reactions (red arrows, mass difference: -5 amu) with pyridine are comparable with that of the association reaction to form $[(\text{Py}^{\text{D}})_2(\text{Py})\text{ZnOH}]^+$ (green arrow, mass

difference: $+79$ amu). In marked contrast, for the complexes with acetate and acetohydroxamate counterions, the exchange reactions are much faster than association. In fact, for the latter complexes, we see association only with the fully exchanged pyridine ligands (mass difference: $+(79-5-5)$ amu), because these complexes underwent the most collisions and are therefore thermalized and consequently can undergo the association most efficiently.³¹ The dominant ions in the manifold of complexes with three ligands are thus $[(\text{Py})_3\text{ZnX}]^+$ ($\text{X} = \text{CH}_3\text{COO}$ or CH_3CONHO) rather than $[(\text{Py}^{\text{D}})_2(\text{Py})\text{ZnX}]^+$, as observed for $\text{X} = \text{OH}$.

The situation is analogous at the larger pressure (Figure 2b). For the zinc–acetate and zinc–acetohydroxamate complexes, the association with pyridine proceeds mostly after the complete exchange of pyridine ligands in the complexes. Consequently, the spectra of association products are dominated by $[(\text{Py})_3\text{ZnX}]^+$, as observed also at the lower pressure. For the zinc–hydroxide complex, there is a pronounced competition between ligand exchange and association, which is reflected in the spectrum by the observation of three peaks corresponding to $[(\text{Py}^{\text{D}})_2(\text{Py})\text{ZnOH}]^+$, $[(\text{Py}^{\text{D}})(\text{Py})_2\text{ZnOH}]^+$, and $[(\text{Py})_3\text{ZnOH}]^+$ with similar abundance.

A comparison of the reactivities of complexes with three ligands $[(\text{Py}^{\text{D}})_3\text{ZnX}]^+$ ($\text{X} = \text{OH}$, Cl, and CH_3COO) first demonstrates that $[(\text{Py}^{\text{D}})_3\text{ZnOH}]^+$ and $[(\text{Py}^{\text{D}})_3\text{ZnCl}]^+$ react analogously (Figure 3). Second, the zinc–acetate complex is again distinctly different from the complexes with monodentate counterions. The ligand-exchange reactions of the zinc–chloride and zinc–hydroxide complexes (red arrows) proceed much faster than the elimination of a ligand (blue arrows). The reactivity of the zinc–acetate complex at the lower pressure (Figure 3a) clearly shows that the exchange reaction is in competition with the ligand elimination. The pattern of the zinc–acetate complex with three pyridine ligands at the higher pressure (Figure 3b) demonstrates the consequence of all of the findings discussed above. Thus, the ligand dissociation is in competition with the exchange reaction. As soon as one pyridine ligand is eliminated, the exchange reaction for the $[(\text{Py}^{\text{D}})_2\text{Zn}(\text{CH}_3\text{COO})]^+$ complex proceeds faster than association, and consequently, the association occurs dominantly for the complex with completely exchanged pyridine ligands. As a result, the $[(\text{Py})_3\text{Zn}(\text{CH}_3\text{COO})]^+$ ion is much more abundant than $[(\text{Py}^{\text{D}})(\text{Py})_2\text{Zn}(\text{CH}_3\text{COO})]^+$.

These findings thus demonstrate that zinc–acetate complexes $[\text{L}_3\text{Zn}(\text{CH}_3\text{COO})]^+$ show a special reactivity mode, which can be referred to as a dissociation–association mechanism. Upon the elimination of one ligand (the dissociation step), a reactive

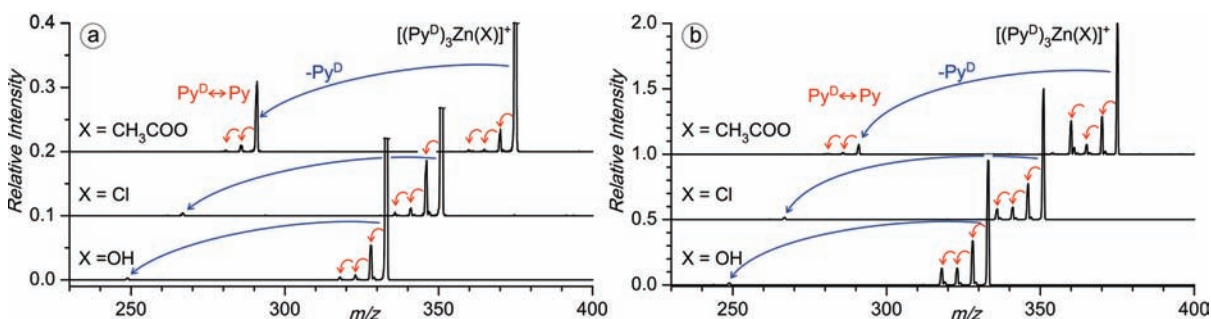


Figure 3. Reaction between $[(\text{Py}^{\text{D}})_3\text{ZnX}]^+$ ($X = \text{OH}, \text{Cl}, \text{and } \text{CH}_3\text{COO}$) and unlabeled pyridine at (a) a lower pressure ($p_{\text{Py}} \sim 0.01$ mtorr) and (b) a higher pressure ($p_{\text{Py}} \sim 0.1$ mtorr). The spectra were normalized by setting the parent-ion intensity to 1.0 (note that the parent peaks in part a are off scale).

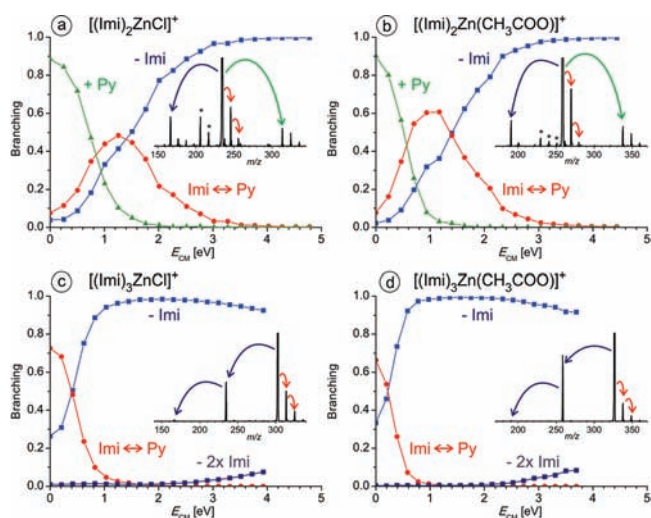
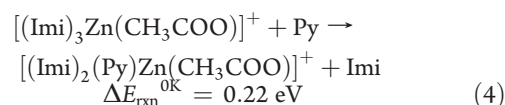
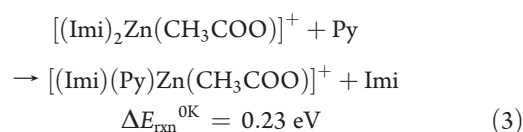
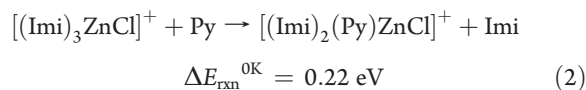
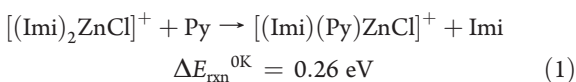


Figure 4. Branching ratios between a loss of imidazole (in blue), the addition of pyridine (in green), and an exchange of imidazole by pyridine (in red) in reactions of (a) $[(\text{Imi})_2\text{ZnCl}]^+$, (b) $[(\text{Imi})_2\text{Zn}(\text{CH}_3\text{COO})]^+$, (c) $[(\text{Imi})_3\text{ZnCl}]^+$, and (d) $[(\text{Imi})_3\text{Zn}(\text{CH}_3\text{COO})]^+$ with pyridine ($p_{\text{Py}} \sim 0.3$ mtorr) dependent on collision energy. The insets show spectra at $E_{\text{CM}} = 1$ eV (a,b; the stars denote peaks originating from an isobaric impurity) or $E_{\text{CM}} = 0.4$ eV (c,d). Note that parent peaks are off-scale. The relative cross sections as well as the results at a lower pressure of pyridine can be found in the Supporting Information.

form of the complex is generated, $[\text{L}_2\text{Zn}(\text{CH}_3\text{COO})]^+$, which can easily attach and again detach other ligand molecules due to the carboxylate shift of the acetate counterion and consequently efficiently mediate ligand-exchange reactions. The reaction pathway is completed by final association of a ligand back to the manifold $[\text{L}_3\text{Zn}(\text{CH}_3\text{COO})]^+$.

The reactivity of complexes with imidazole ligands ($[(\text{Imi})_n\text{ZnX}]^+$, where $X = \text{Cl}$ or CH_3COO and $n = 2$ or 3) with pyridine was also studied (Figure 4). The theoretical investigation of the $[(\text{Imi})_n(\text{Py})_m\text{ZnX}]^+$ ($m = 0, 1$) complexes reveals that the exchange of imidazole by pyridine in the complexes is an endothermic process (see reactions 1–4). The energy required is slightly larger than 0.2 eV for all complexes investigated.



The endothermicity of the exchange reaction implies that collision energies larger than zero will be required in order to promote the exchange reaction. The association of the ligands is only efficient at collision energies close to zero, and therefore the dissociation–association mechanism for the ligand exchange, which is important in the reactivity of acetates as demonstrated above, should be switched off.

Figure 4 shows branching ratios between the association (in green), the dissociation (in blue), and the exchange reactions (in red). The $[(\text{Imi})_2\text{ZnX}]^+$ complexes (Figure 4a and b) react analogously regardless of whether the counterion X is chloride or acetate. The association of $[(\text{Imi})_2\text{ZnX}]^+$ with pyridine prevails at zero collision energy, whereas large collision energies lead almost exclusively to the elimination of imidazole. The exchange of imidazole by pyridine is most important at collision energies slightly above 1 eV. At low pressures of pyridine, only the exchange of one imidazole molecule is observed (Figures S4 and S5 in the Supporting Information); at larger pressures, both ligands can be exchanged (shown here). The insets in Figure 4a and b show the spectra at collision energies of about 1 eV. Evidently, there are no major differences in reactivity of $[(\text{Imi})_2\text{ZnCl}]^+$ and $[(\text{Imi})_2\text{Zn}(\text{CH}_3\text{COO})]^+$. In comparison with the thermoneutral exchange reactions studied for the pyridine complexes above, the reactivity pattern can be compared with that of $[(\text{Py}^{\text{D}})_2\text{ZnCl}]^+$ (Figure 2). The association reaction at low collision energies is faster than the exchange reaction; hence the dominant ion with three ligands corresponds to $[(\text{Py})(\text{Imi})_2\text{ZnX}]^+$ and not to $[(\text{Py})_3\text{ZnX}]^+$, which would be expected, if the exchange reaction were faster (compare with Figure 2). Consequently, the fast reactivity mode of the complex with two ligands and the acetate counterion observed for the

Table 1. Theoretical Bonding Energies of Ligand L (L = Imi or Py) in Complexes $[\text{ZnX}(\text{L})_n]^+$ (X = Cl or CH_3COO , and $n = 2$ or 3)

	$\text{BE}_{\text{theor}} [\text{eV}]$	
	L = Imi	L = Py
$[\text{L}_2\text{Zn}(\text{CH}_3\text{COO})]^+$	1.93	1.74
$[\text{L}_2\text{ZnCl}]^+$	2.09	1.84
$[\text{L}_3\text{Zn}(\text{CH}_3\text{COO})]^+$	1.19	0.93
$[\text{L}_3\text{ZnCl}]^+$	1.44	1.29

thermoneutral reaction with L = Py is switched off, if the reaction is endothermic, as in the case with L = Imi.

The complexes with three ligands, $[(\text{Imi})_3\text{ZnCl}]^+$ and $[(\text{Imi})_3\text{Zn}(\text{CH}_3\text{COO})]^+$, also show very similar reactivity patterns. The exchange reaction dominates at collision energies close to zero, but already at collision energies below 1 eV, the elimination of one of the imidazole ligands starts to prevail. The reactivity pattern of both complexes can be compared to that of $[(\text{Py})_3\text{ZnCl}]^+$, and the special reactivity feature of the zinc–acetate complex, which employs the efficient exchange reaction at the $[(\text{L})_2\text{Zn}(\text{CH}_3\text{COO})]^+$ stage, is lost, because the association step does not proceed at larger collision energies.

A comparison of the dissociation patterns of $[(\text{Imi})_3\text{ZnCl}]^+$ and $[(\text{Imi})_3\text{Zn}(\text{CH}_3\text{COO})]^+$ suggests a substantial difference between the binding energies of the third imidazole ligand (see Table 1). We have therefore also calculated bonding energies of imidazole in complexes $[(\text{Imi})_n\text{ZnX}]^+$ and pyridine in complexes $[(\text{Py})_n\text{ZnX}]^+$ (X = Cl or CH_3COO and $n = 2$ or 3). The results suggest that the binding energy of the second ligand to the $[(\text{L})\text{ZnX}]^+$ core differs depending on the counterion by about 0.1 to 0.2 eV (roughly 10% of the binding energy). The counterions have, however, larger effects, if the complexes bear three ligands. The differences between the binding energies of the third ligand are on the order of 0.3 eV, which represents roughly 25% of the binding energy. The larger lability of the third ligand in the zinc–acetate complexes is a direct consequence of the coordination change of the acetate counterion and once more demonstrates the effect of the carboxylate shift on the reactivity of zinc–acetate complexes. The energy dependence of the experimental relative cross sections for ligand eliminations can be found in the Supporting Information (Figure S6).

CONCLUSIONS

Infrared multiphoton dissociation spectroscopy unambiguously reveals a pronounced change of the coordination mode of the acetate ligand in complexes $[(\text{Imi})_n\text{Zn}(\text{CH}_3\text{COO})]^+$ ($n = 1–3$) dependent on the number of ligands n .³² While acetate acts as a bidentate ligand in the complexes with one and two imidazole ligands, its coordination changes to monodentate once a third imidazole ligand is attached. This behavior is a direct gas-phase mimic of the “carboxylate shift” referred to in biochemistry. We have further investigated the effect of the coordination of the carboxylate ligand on the reactivity of zinc–acetate complexes in comparison with those bearing different counterions. In the reaction of complexes $[(\text{Py}^{\text{D}})_n\text{ZnX}]^+$ ($\text{Py}^{\text{D}} = \text{D}_5\text{-pyridine}$, X = Cl, OH, CH_3COO , or CH_3CONHO , and $n = 2$ or 3) with unlabeled pyridine, the carboxylate shift crucially influences the reactivity of zinc–acetate complexes, whereas the effect is absent for the other counterions. Complexes $[\text{L}_3\text{ZnX}]^+$

with monodentate counterions X (i.e., hydroxide or chloride) react with other molecules L simply by an association–dissociation mechanism. On the other hand, a facile elimination of the ligand L due to the carboxylate shift in the $[\text{L}_3\text{Zn}(\text{CH}_3\text{COO})]^+$ complexes opens a more effective channel, in which a faster association–dissociation reaction proceeds in the $[\text{L}_2\text{Zn}(\text{CH}_3\text{COO})]^+$ stage.

ASSOCIATED CONTENT

S Supporting Information. Total energies, optimized geometries, dependence of free-electron laser intensity on the wavelength during measurements, more spectra from the reactivity study, and complete ref 22. This information is available free of charge via the Internet at <http://pubs.acs.org/>.

AUTHOR INFORMATION

Corresponding Author

*E-mail: roithova@natur.cuni.cz.

ACKNOWLEDGMENT

The authors thank the Grant Agency of the Czech Republic (203/08/1487), the Ministry of Education of the Czech Republic (MSM0021620857), and the European Commission for travel grants to the European multiuser facility CLIO. The authors would like to thank Joël Lemaire and Vincent Steinmetz for their kind assistance during the measurements at CLIO.

REFERENCES

- (1) Lipscomb, W. N.; Sträter, N. *Chem. Rev.* **1996**, *96*, 2375.
- (2) Auld, D. S. *Biomaterials* **2001**, *14*, 271.
- (3) Maret, W.; Li, Y. *Chem. Rev.* **2009**, *109*, 4682.
- (4) (a) Christianson, D. W.; Lipscomb, W. N. *Acc. Chem. Res.* **1989**, *22*, 62.
- (5) Sousa, S. F.; Pedro, A.; Fernandes, P. A.; Ramos, M. J. *J. Am. Chem. Soc.* **2007**, *129*, 1378.
- (6) Dudev, T.; Carmay, L. *Acc. Chem. Res.* **2007**, *40*, 85.
- (7) Ryde, U. *Biophys. J.* **1999**, *77*, 2777.
- (8) (a) Mhin, B. J.; Lee, S.; Cho, S. J.; Lee, K.; Kim, K. S. *Chem. Phys. Lett.* **1992**, *197*, 77. (b) Lee, S.; Kim, J.; Park, J. K.; Kim, K. S. *J. Phys. Chem.* **1996**, *100*, 14329. (c) Pavlova, M.; Siegbahn, P. E. M.; Sandström, M. *J. Phys. Chem. A* **1998**, *102*, 219. (d) Mohammed, A. M.; Loeffler, H. H.; Inada, Y.; Tanada, K.; Funahashi, S. *J. Mol. Liq.* **2005**, *119*, 55. (e) Bernasconi, L.; Baerends, E. J.; Sprik, M. *J. Phys. Chem. B* **2006**, *110*, 11444. (f) De, S.; Ali, S. K. M.; Alib, A.; Gaikar, V. G. *Phys. Chem. Chem. Phys.* **2009**, *11*, 8285.
- (9) Fatmi, M. Q.; Hoferb, T. S.; Rode, B. M. *Phys. Chem. Chem. Phys.* **2010**, *12*, 9713.
- (10) Chen, X.; Wu, G.; Wu, B.; Duncombe, B. J.; Stace, A. J. *J. Phys. Chem. B* **2008**, *112*, 15525.
- (11) Zhu, M.; Pan, G. *J. Phys. Chem. A* **2005**, *109*, 7648.
- (12) (a) Parkin, G. *Chem. Commun.* **2000**, 1971. (b) Parkin, G. *Chem. Rev.* **2004**, *104*, 699.
- (13) Ducháčková, L.; Roithová, J. *Chem.—Eur. J.* **2009**, *15*, 13399.
- (14) Ricketts, C. L.; Schröder, D.; Roithová, J.; Schwarz, H.; Thissen, R.; Dutuit, O.; Žabka, J.; Herman, Z.; Price, S. D. *Phys. Chem. Chem. Phys.* **2008**, *10*, 5135.
- (15) For examples of postsource thermalization in ESI, see: (a) Hinderling, C.; Feichtinger, D.; Plattner, D. A.; Chen, P. *J. Am. Chem. Soc.* **1997**, *119*, 10793. (b) Moision, R. M.; Armentrout, P. B. *J. Am. Soc. Mass Spectrom.* **2007**, *18*, 1124.
- (16) Mac Aleese, L.; Simon, A.; McMahon, T. B.; Ortega, J. M.; Scuderi, D.; Lemaire, J.; Maitre, P. *Int. J. Mass Spectrom.* **2006**, *249*, 14.

- (17) Ramos, M. J.; Fernandes, P. A. *Acc. Chem. Res.* **2008**, *41*, 689.
- (18) Vosko, S. H.; Wilk, L.; Nusair, M. *Can. J. Phys.* **1980**, *58*, 1200.
- (19) Lee, C.; Yang, W.; Parr, R. G. *Phys. Rev. B* **1988**, *37*, 785.
- (20) Becke, A. D. *Phys. Rev. A* **1988**, *38*, 3098.
- (21) Becke, A. D. *J. Chem. Phys.* **1993**, *98*, 5648.
- (22) Frisch, M. J. et al. *Gaussian 03*, revision C.02; Gaussian, Inc.: Wallingford, CT, 2004.
- (23) For the method B3LYP/6-311+G(d,p), a scaling factor of 0.9688 is suggested in work: Merrick, J. P.; Moran, D.; Radom, L. *J. Phys. Chem. A* **2007**, *111*, 11683. This scaling, however, leads to a worse agreement with the experimental spectra of the zinc complexes studied here.
- (24) Wagner, M.; Limberg, C. *Inorg. Chim. Acta* **2009**, *362*, 4809.
- (25) Višnjevac, A.; Gout, J.; Ingert, N.; Bistri, O.; Reinaud, O. *Org. Lett.* **2010**, *12*, 2044.
- (26) (a) Talaei, Z.; Morsali, A.; Mahjoub, A. R. *Z. Naturforsch. Sect. B, Chem. Sci.* **2005**, *60*, 1049. (b) Kumar, U.; Thomas, J.; Thirupathi, N. *Inorg. Chem.* **2010**, *49*, 62.
- (27) For a recent report about possibly pentacoordinated zinc in $[\text{Zn}(\text{H}_2\text{O})_n]^{2+}$ dications, see: Cooper, T.; O'Brien, J. T.; Williams, E. R.; Armentrout, P. B. *J. Phys. Chem. A* **2011**, in press (10.1021/jp1078345).
- (28) Groenewold, G. S.; de Jong, W. A.; Oomens, J.; Van Stipdonk, M. J. *J. Am. Soc. Mass Spectrom.* **2010**, *21*, 719.
- (29) Schröder, D.; Schwarz, H.; Schenk, S.; Anders, E. *Angew. Chem., Int. Ed.* **2003**, *42*, 5087.
- (30) Cood, R. *Coord. Chem. Rev.* **2008**, *252*, 1387.
- (31) Jagoda-Cwiklik, B.; Jungwirth, P.; Rulišek, L.; Milko, P.; Roithová, J.; Lemaire, J.; Maitre, P.; Ortega, J. M.; Schröder, D. *ChemPhysChem* **2007**, *8*, 1629.
- (32) For a conceptually related effect of the number of ligands on the spin distribution in copper(II) complexes, see: Milko, P.; Roithová, J.; Tsierkezos, N. G.; Schröder, D. *J. Am. Chem. Soc.* **2008**, *130*, 7186.